MAGNETIC AND STRUCTURAL STUDIES OF Co-Al THIN FILMS AND BULK ALLOYS

by

A. G. TSOUKATOS

B.S., Concordia University, 1984
M.S., University of Manitoba,1986

———————————

A THESIS

submitted in fulfillment of the

requirements for the degree

MASTER OF SCIENCE

PHYSICS

KANSAS STATE UNIVERSITY
Manhattan , Kansas

1988

Approved by:

George Hadjipanayis

Major Professor

TABLE OF CONTENTS

i

ACKNOWLEDGEMENTS

I would like to thank my supervisor, Dr. G. Hadjipanayis, for introducing me to this project, and also for his support while I was working on this project . I would also like to thank Dr. B. Dale for his continuous help and encouragement during the course of this project.

Special thanks are also due to Dr. J. Strzeszewski and Mr. L. Seib for their help in the accomplishment of this work .

Finally, I would like to thank my husband for his help and support during the course of this work .

ABSTRACT

Thin films of $Co_{100-x}Al_x$ were prepared by co-evaporation. The as-deposited films had the hexagonal Co structure for $x \leq 25$, a disordered bcc-CoAl structure for x=30, and a partially ordered bcc-CoAl structure for $x \geq 30$. After heat treatment at 650^0C the films with $x \leq 25$ changed microstructure to fine mixture of hcp-Co and an ordered fcc structure which may be interpreted as Co_3Al. Films with $25 \leq x \leq 50$ were transformed to ordered fcc- Co_3Al and bcc-CoAl structures after the heat treatment. The magnetization of the films was greater than that for bulk alloys with the same composition and it decreased when the films were annealed at 650^0C. The finely distributed two phase microstructure is probably responsible for the observed coercivity (50-150 Oe).

Ribbons of Co-Al were prepared by melt-spinning. The as melt-spun ribbons had a mixture of phases with a strong hcp-Co structure for $x \leq 25$, and strong hcp-Co and fcc-Co for $x \geq 25$. Co-rich phases continue to exist along with the Co_3Al phase in all of the compositions studied. The magnetization and coercivity values were comparable to those of bulk Co-Al of similar composition . The relatively high coercivities observed are attributed to the complex crystal structure found in all of the Co-Al ribbons.

1. INTRODUCTION

1.1 Thin Films

The term metallic thin films referrs to the metallic layers whose thickness ranges from a few atomic diameters to a few hundred angstroms. Thin films have been investigated since the middle of the 1900's [1], but , the study of their magnetic behavior has been recently reconsidered largely because of their potential application in memory devices such as magnetic disks. Furthermore, this field of study can itself create pure scientific interest due to the complex nature it presents concerning the magnetic and structural properties of the films.

The study of the fundamentals of thin film formation and the essential differences between thin films and bulk materials of the same composition is extremely important from the scientific point of view as well as for the technological advances that may result from these findings.

Thin films can be prepared by electrolytic deposition, by sputtering and by vacuum evaporation [1,2]. The most commonly used methods are sputtering and vacuum evaporation from heated sources. The method of vacuum evaporation was used for the preparation of the thin films studied in this project.

Vacuum deposition of films is obtained under very low pressure by thermally evaporating the source material onto the substrate. A variety of evaporation boats can be used, which are made of refractory metals, such as tantalum, tungsten, or molybdenum, that are coveniently heated by passing a current through them. The choice of such a boat depends on the properties of the evaporant, that is, whether it dissolves the boat material or if it its melting point and evaporation temperature are higher than those of the boat material. It should also be noted, that source materials can be heated to evaporation by electron bombardment using a focused

1

electron gun assembly, or by the use of a high power laser which is usually positioned outside the vacuum system [2].

One of the setbacks in thin film studies has been the reproducibility of the film properties for some the systems studied [2]. However, the constant control and improvement of the preparation techniques has resulted in a more standardized production of thin films , that allows their use even in some commercial applications. Nevertheless, some discrepancies are still encountered, and a totally controlled method for the preparation of thin films is yet to be achieved, and to date, it can only be approached in well equiped laboratories under clean room conditions.

1.2 Melt-spun materials

Melt-spun materials, in the form of ribbons, result from the solidification of a molten material by means of a melt-spinning device . The solidification of the liquid material may happen in two ways: the liquid may solidify in a discontinuous manner to a crystalline solid, or, it may solidify in a continuous manner to an amorphous solid.

The specific form of solidification depends on the method used to achieve such a solid. The transition from the liquid state to the crystal state occurs when the cooling rate during quenching is sufficiently low. That is, there is an abrupt contraction in the volume of the crystal which occurs by quenching from the melting temperature point. On the other hand if the quenching is very rapid, that is, if it occurs at very high cooling rates, then the liquid phase continues to exist past the freezing point, until a lower temperature, which is known as the glass transition temperature, where solidification occurs in the amorphous state [3,4]. The difference between crystal and amorphous solids is that the former exhibit a long range order (periodicity) in the equilibrium positions of the atoms, while the latter have a non-periodic structure. The solidification of liquid into amorphous solids is an

almost universal property of solids [3]. However, the final form of a solid depends on the conditions during quenching, that is the rate of cooling of the liquid, and the uniformity of the molten material.

In this work, Co-Al ribbons were prepared in a melt spinning device. This method of ribbon preparation is appropriate for obtaining amorphous solids. The main features of the apparatus used for the ribbon preparation is shown in Figure 1.1, and the ribbon is obtained by forcing the liquid alloy onto the spinning wheel by applying gas pressure on it (as indicated by the figure). The resulting solid can be of either form, i.e. crystal or amorphous, depending on the conditions under which the liquid solidifies.

The Co-Al ribbons were prepared at high cooling rates but their resulting structure was crystalline. This is possibly due to the fact that this alloy does not have the property known as "glass- forming tendency " [3]. The lack of this property can be explained by considering the components of this Co-Al alloy. It is well known that the melting temperature of each component has a different value, so that the liquid state of each of them is approached at different times. Therefore, a heterogeneous liquid state is obtained which leads to crystallization of the resulting ribbon, while it is known that the formation of an amorphous material follows a homogeneous transition process [3,4].

1.3 Magnetic Hysteresis

In the study of the magnetic behavior of thin films the most interesting property is that of coercivity H_c (in Oe). The values of coercivity are obtained from the measured hysteresis loops. The hysteresis or irreversibility is a property of magnetic materials, according to which, after saturation, a decrease of the magnetic field to zero does not cause the magnetization to return to zero. Figure 1.2 shows an idealized hysteresis loop in terms of magnetization, M, magnetic induction, B, and

Figure 1.1 : The basic features of a melt-spinning device consist of a spinning Cu wheel, a sample holder that can be heated, and an Ar gas system that allows the sample preparation without any oxidization taking place. (Zallen [3])
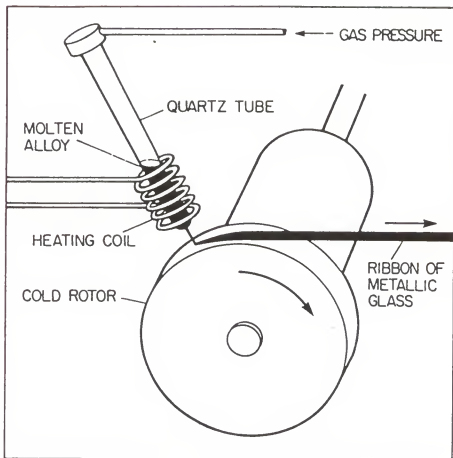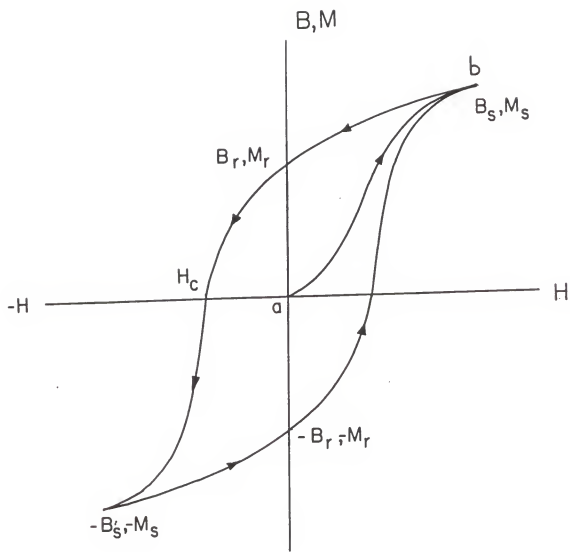
GAS PRESSURE

QUARTZ TUBE

MOLTEN
ALLOY

HEATING COIL

COLD ROTOR

RIBBON OF
METALLIC
GLASS

Figure 1.2 : An idealized hysteresis loop as a function of magnetization, M, magnetic induction, B, and the applied magnetic field, H.

5a

the applied magnetic field, H, in order to be able to point out the specifics of such a measurement and the associated theoretical models that have been developed to explain this behavior of magnetic materials [5,6].

The curve ab, from zero (the demagnetized state) to saturation is called the initial or normal induction curve. When the applied field, H, is reduced to zero from saturation, the magnetization, M, and the magnetic induction, B, will not reduce to zero but to the lower values of M_r, and B_r, which are called the remanent magnetization and the residual induction, respectively. If the polarity of the applied field, H, is reversed, the magnetic induction and the magnetization are reduced to zero when the negative field attains the coercivity value, H_c. This coercivity value is known as the field necessary to reduce the magnetization to zero, and is called the intrinsic magnetization. By further increasing the applied field one obtains the negative saturation values of B and M. Continuation of the cycle through zero to saturation traces out a loop known as the major hysteresis loop . If the applied field is not large enough to saturate the specimen, then a minor hysteresis loop is obtained instead.

For thin films the magnetization orientation and reversal is obtained by domain wall motion in the lower fields and by rotation in the higher fields [5,6,7,8]. A similar behavior is found in bulk material also. The difference between the bulk materials and the thin films is that in thin films the third dimension is reduced so that the demagnetization factor in the plane of the film becomes negligible [2]. One factor that affects the shape of the hysteresis loop is the magnetic anisotropy. There are several types of magnetic anisotropy, such as crystalline anisotropy, shape anisotropy, etc., the most important of all being the crystal anisotropy, which is an intrinsic property of the material, while all others are induced [5,6]. The magnetic anisotropy indicates that the properties of a magnetic material depend on the orientation in which they are measured. Crystal anisotropy originates from the spin-orbit interactions and its strength is measured by the magnitude of the anisotropy constants.

The explanation of magnetic hysteresis has been attempted by various theoret-

ical models. Two of the most respectable theoretical models used for the explanation of hysteresis, are the single domain particle model and the domain wall pinning model.

In relation to the single domain particle model [5,6,7,8], it has been found that, below a critical diameter the particles in a magnetic material become single domains, whose magnetization is changed by spin rotation. There are various types of rotation that can happen, such as coherent, incoherent, etc.. A rotation is considered to be coherent if all the spins rotate uniformly, while a rotation is termed incoherent if the spin rotation is non-uniform. The domain wall pinning model [5,6,7,8] describes the change in magnetization through the motion of the domain walls. Domain wall motion is sometimes hindered by imperfections in the crystal. The domain walls are then said to be pinned. The unpinning of domain walls, that is total magnetization reversal, is affected by two forces that act on the domain wall. One of the forces attempts to unpin the wall, while the other tries to keep it pinned. The former force results from the applied magnetic field, and the latter from the imperfection.

Finally, it should be noted that the application of the these models to explain the magnetic hysteresis and coercivity of the various types of materials needs to be adjusted for the conditions describing each of the materials.

1.4 $Co_{100-x}Al_x$ Thin Films

1.4.1 An overview of the subject

Co-Al alloys in bulk form have been extensively studied because of the relatively high coercivities they exhibit [9to15]. As-cast Co-Al alloys become magnetically hard after an appropriate heat treatments in the temperature range of 500^0 C to 700^0 C. However, very little work has been done on Co-Al thin films [10]. Most of the work on Co-transition metal thin films has been devoted to the CoCr system because of its promising behavior regarding its application in computer technology i.e., high density storage through perpendicular recording [16to21].

7

As mentioned previously , Co-Al alloys in bulk form have exhibited very intertesting magnetic properties with high coercivities that have been attributed to single domain particles of Co, which are assumed to have precipitated in a CoAl matrix[9,10,15] .These results were obtained from Co rich bulk alloys and it was part of this work to determine whether a similar behavior was observed in Co-rich thin films.

It has been reported [14] that Al-rich Co-Al thin films prepared by rf sputtering have an amorphous structure with fcc Al crystallites found in the amorphous matrix. The same study also reports that for the Al rich compositions there are many intermetallic compounds such as Co_2Al_9, Co_4Al_{13}, etc.,along with the amorphous phase . The amorphous phase is always observed if the composition ranges between75% and 90% at. Al. Co-rich compositions with more than 20% at. Al and less than or equal to 50% at. Al have been found to have a microcrystalline structure which is a mixture of two phases one of which is magnetic, or consists of a magnetic fcc or hcp phase depending on the Al content. The magnetic behavior of these Al rich films has not been discussed since their Al rich structure is highly non magnetic .

1.4.2 Focus of this project

In the previous sections the subject of thin films ,their methods of preparation and the specific topic of Co-Al thin films and bulk alloys were briefly discussed in order to be able to focus on the work performed for this project and generally , provide some insight on the reasons that iniciated this work.

The initial idea regarding this project was to study Co rich Co-Al thin films of various chemical compositions in order to find out whether they would exhibit the high coercivity and perpendicular anisotropy that would make them candidates for perpendicular magnetic recording. Furthermore, their microstructure was to

be studied and correlated to their magnetic properties in order to understand the origin of coercivity in these materials. The information regarding the properties of Co rich bulk alloys of Co-Al was also going to be compared to that obtained for thin films of similar compositions in order to point out the similarities and/or the differences in the properties of the bulk material and those of the thin films.

Overall, this project should be considered as an effort to clarify the differences between bulk alloys and thin films of the same chemical composition and also to determine whether this Co-transition metal binary alloys could be good candidates for commercial applications in perpendicular recording.

The presentation of this work will continue as follows. In Chapter 2, the experimental techniques for the preparation of bulk alloys, ribbons, and films will be discussed along with the methods of studying their magnetic and structural properties. In Chapter 3 the data obtained will be presented. In Chapter 4 a discussion of the data obtained will be made and there will be an effort to explain the results obtained with respect to the existing theoretical models. Finally, Chapter 5 will involve the concluding remarks on this project.

2. EXPERIMENTAL METHODS

2.1 Specimen preparation techniques

### 2.1.1 $Co_{100-x}Al_x$ Thin films by vacuum evaporation

Thin films of several metals can be prepared by evaporation from refractory metal supports in vacuum under controlled conditions. The apparatus used for the thin film preparation consists of two major parts, the pumping system and the coating chamber. The pumping system consists of a mechanical and an ion pump. Possible backstreaming from the mechanical pump is avoided by inserting a sorption trap between the mechanical pump and the coating chamber, and in this way the coating chamber remains free of oil contamination. The coating chamber is equipped with removable components so as to allow flexibility in the arrangement of the experimental set up required for the different evaporations.

The Co-Al thin films for this work were prepared by coevaporation; that is, the metals were placed in separate evaporation crucibles, which were then positioned appropriately so as to obtain the uniformly deposited binary alloys of Co and Al. The geometry of the evaporation set up is very important since it is closely related to the sample thickness uniformity, its chemical composition, and possibly the crystal structure of the resulting thin film [1,2,22]. Figure 2.1 shows a schematic diagram of the evaporation setup, which was used to obtain the Co-Al thin films. This setup was kept the same throughout all the evaporations in order to make possible the comparison of the resulting thin films in terms of the factors mentioned above.

A simple minded approach of the evaporation process, from the theoretical point of view would be to consider the evaporation sourse as a point source which evaporates the material at an equal rate in all directions [1]. The amount of material, dm, passing through a solid angle, $d\Omega$, is

$$dm = \frac{m}{4\pi} \cdot d\Omega \quad . \tag{1}$$

Figure 2.1 : A schematic diagram of the evaporation set up used for the preparation of Co-Al thin films; S_1, S_2= evaporation sources, G= glass substrates, M= mica substrate, S= NaCl substrate.
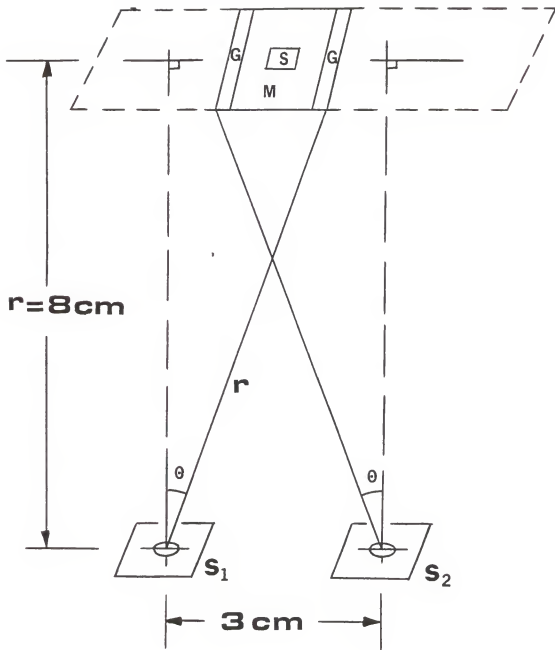
where m= the total mass evaporated

The amount of mass, dm, is the same in any direction per unit time.

Figure 2.2a shows a schematic diagram of the point source concept described above.

The Co and Al evaporants were deposited on substrates which were positioned parallel to the surface of the "point sources ", that is ,the direction of the vapor stream was at an angle, θ ,with the normal of the receiving surface dS' (see Figure 2.2b). Therefore the amount of the deposited material and its thickness are calculated as follows :

$$d\Omega = \frac{cos\theta}{r^2} \cdot dS' \quad . \tag{2}$$

where r is in the direction of vapor flow

From equations (1) and (2) we obtain :

$$dm = \frac{m}{4\pi} \cdot \frac{cos\theta}{r^2} \cdot dS' \quad . \tag{3}$$

For the thickness calculation the following is considered:

$$dm = (density, \rho) \cdot (thickness, t) \cdot dS' \quad . \tag{4}$$

From equations (3) and (4) follows:

$$t = \frac{m}{4\pi \cdot \rho} \cdot \frac{cos\theta}{r^2} = \frac{V}{4\pi} \cdot \frac{cos\theta}{r^2} \quad . \tag{5}$$
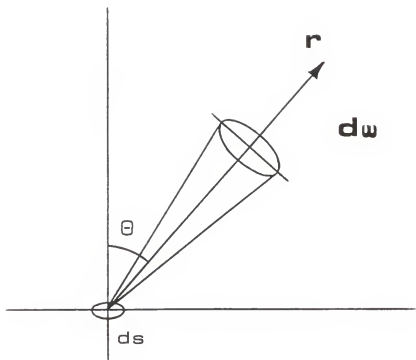
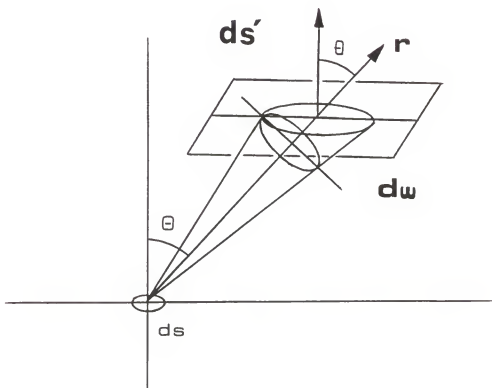where V= the total volume evaporated

Also , it should be noted that

$$r_0 = r \cdot cos\theta \quad . \tag{6}$$

12

Figure 2.2 : Schematic represantation of a point source configuration; (a).the mass is evaporated at an equal rate onto the inner surface of a virtual sphere (b).a receiving surface is placed parallel to the point source so as to make an angle with the direction of the vapor stream.

From equations (5) and (6) follows:

$$t = \frac{V}{4\pi \cdot r_0^2} \cdot cos^3\theta \quad .$$ (7)

Equation (7) describes a relation for the thickness determination , which was used to approximate the variation per centimetre of length of the substrate. The thickness was found to vary by approximately $4.5\%/cm$.

To avoid great variations in the film thickness and the chemical composition (considering that there were two "point sources" involved in the evaporation) the total substrate length was contained within 2cm (see Figure 2.1 for dimensions).

Three different kinds of substrate were used : rock salt (NaCl), mica, and glass. The thin films evaporated on NaCl were used for electron microscopy studies , while those on mica were used for magnetic measurements. Finally, the thin films evporated on glass were used for thickness measurements using an optical interference method which applies the Fizeau fringes of equal thickness principle [1,22]. The film thicknesses measured using this method ranged between 900 A and 1000 A.

Other important factors influencing the film formation are, the substrate temperature, the substrate surface contamination, and the rate of evaporation. It has been shown experimentally [1,2] that low temperature (cooled) substrates contribute in the formation of amorphous thin films, while heated substrates favor the formation of crystalline thin films. The Co-Al thin films were prepared at room temperature , with their substrates occasionally registering temperatures above room temperature due to heating from the evaporating element.

Contaminated surfaces inside the the coating chamber will result in poor vacuum. Furthermore, contamination of the substrate surface by water , grease, or any other substance may result in an oxidized film, or poor adherence on the substrate and in general a thin film that cannot be used for experimental purposes. The rate of evaporation during the deposition of a thin film needs to be adjusted so as to

avoid overly long term evaporations which lower the vacuum and thus lead to the oxidization of the deposited film.

For the Co-Al thin films the rate of evaporation of each evaporant was adjusted in order to obtain the various chemical compositions required. The different evaporation rates were monitored with respect to the resistivity of each evaporant which was plotted out during the evaporation and thus the respective rates were controlled so as to obtain the desired composition. Finally, it should be noted that the purity of the materials used as evaporants was better than99.9% and that the compositions obtained ranged between x= 20 and x= 50 atomic percent of Al .It should also be noted that the base pressure during coevaporation was maintained at approximately 10^{-6} Torr.

2.1.2 Bulk alloy preparation of $Co_{100-x}Al_x$

Bulk Co-Al alloys were prepared by arc - melting together under Argon atmosphere the amounts of pure Co and Al required for each composition. The presence of the inert atmosphere was required in order to avoid oxidization of the sample. The specimens were weighed before and after melting and there were no significant losses in the amount of the materials (less than .1% total weight loss. These bulk alloys were then sectioned into smaller pieces and used for the characterization of their magnetic behavior .

2.1.3 Ribbon preparation of $Co_{100-x}Al_x$

The Co-Al ribbons were prepared under an Argon atmosphere in a homemade melt- spinning device. The specimen is heated to melting and then ejected onto a spinning wheel , where it is rapidly cooled in the form of ribbons. These ribbons were to be tested in terms of their magnetic properties and their microstructure and then compared to the results obtained for bulk and thin films.

2.2 Characterization of $Co_{100-x}Al_x$

2.2.1 Magnetic measurements

The magnetic measurements of all the specimens were obtained using a vibrating sample magnetometer or a SQUID magnetometer. Samples of known mass were used to obtain the coercivity H_c (Oe), the magnetization M_s (emu/gr), and thermomagnetic behavior of the Co-Al alloys.

Ac susceptibility measurements were obtained for some of the compositions for ribbons and thin films in the temperature range of 4.2^0K to 300^0K.

Co-Al thin films and ribbons were heat treated in the temperature range of 600^0C to 700^0C in order to induce magnetic hardening. The thin films were heat treated for 4 hours at 650^0 C under vacuum and their magnetic behavior was examined afterwards. The ribbons were also heat treated at 650^0 C and under vacuum but their heating times ranged between 8 and 32 hour intervals . The heat treatment of the ribbons was arranged in such a manner as to obtain maximum magnetic hardening.

Because thin films are quite delicate and easily oxidized structures, they were not heat treated to the point of maximum coercivity, even though their heat treatment indicated an increase in the values of the coercivity.

2.2.2 Microstructure measurements

Extensive analytical and structural studies were performed for all the thin film and ribbon specimens studied . The electron microscope evaluation of each thin film specimen began with the chemical composition analysis in order to verify its exact composition. This task was performed with energy dispersive X-ray analysis using a Si-Li detector attached to a Jeol 100C scanning transmission electron microscope. Then, using the same microscope the structural properties, the microstructure and

16

the magnetic domain structure of each specimen were studied before and after the heat treatment. The crystal structure information was obtained through electron diffraction, while the microstructure information was obtained from bright and dark field images. Magnetic domains and magnetic domain wall information were obtained using Lorentz microscopy and were used for further clarification of the structural and magnetic behavior of the thin film specimens. The same information was also gathered for the ribbon specimens before and after the heat treatment for characterization and subsequent comparison with the thin films of the same composition. The ribbon and bulk specimens of the $Co_{100-x}Al_x$ alloys had their X-ray diffraction patterns measured using a filtered Cr source, so that an accurate determination could be obtained. The X-ray diffraction patterns were then matched to the crystal phase determined from the electron diffraction patterns of the electron microscopy studies.

3. DATA COMPILATION FOR $Co_{100-x}Al_x$ ALLOYS

3.1 Magnetic data

3.1.1 The coercivity of thin films, ribbons, and bulk $Co_{100-x}Al_x$ alloys

The hysteresis loops of thin film samples of $Co_{100-x}Al_x$ with $20 \leq x \leq 50$ were measured using a SQUID magnetometer for the best possible accuracy, regarding the small mass involved in each specimen that was measured (Figure 3.1). The coercivities measured for the various compositions are characteristic of soft magnetic materials. They are found to vary between 20 Oe and 150 Oe before heat treatment of the as-deposited films. The specific coercivities obtained for each composition are shown on Figure 3.2 along with the coercivities of bulk alloys and ribbons of the same chemical compositions. The coercivities of the thin films are found to be much lower than those of bulk and ribbon alloys of Co-Al. A possible explanation for such findings is to attribute them to the different microstructure in the films and the bulk and ribbon alloys studied. The thin film coercivities were determined after introducing the samples to magnetizing fields as high as 55 kOe. The coercivities of the ribbons and the bulk samples were obtained after introducing them to magnetic fields of the order of 17 kOe or 55 kOe or both. It is observed here, that the values of coercivity of the as melt spun ribbons are similar to those of bulk, observed for bulk alloys with small variations that could be attributed to the differentiation in microstructure.

The heat treated films showed increased coercivities, but these values were still low, characteristic of relatively soft magnetic materials. This can be attributed to the very fine microstructure of the films which were found to contain magnetically soft cubic phases. Figure 3.3 shows the coercivities of the heat treated films as a function of chemical composition along with the optimized coercivities of the heat treated ribbons.

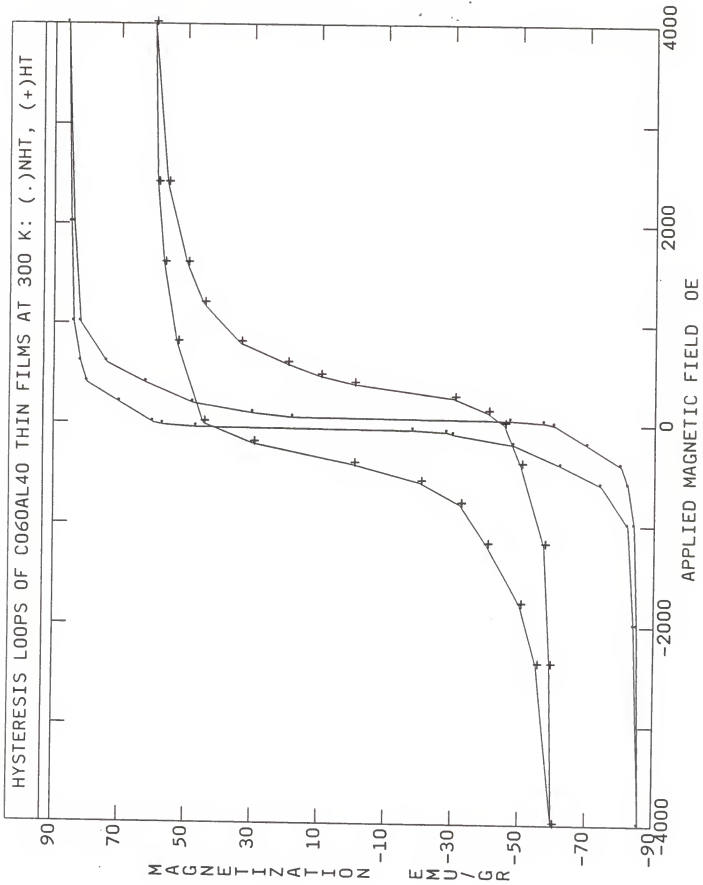Figure 3.1 : Typical hysteresis loops of as-deposited and heat treated (4hrs, 650^0C) $Co_{60}Al_{40}$ thin films.

HYSTERESIS LOOPS OF CO60AL40 THIN FILMS AT 300 K: (.)NHT, (+)HT

19a

Figure 3.2 : Coercive fields of Co-Al alloys; as-deposited thin films, as melt-spun ribbons, and as-cast bulk.

(.)BULK, (+)RIBBONS, (X)FILMS: AT 300 K, NON-HEAT TREATED
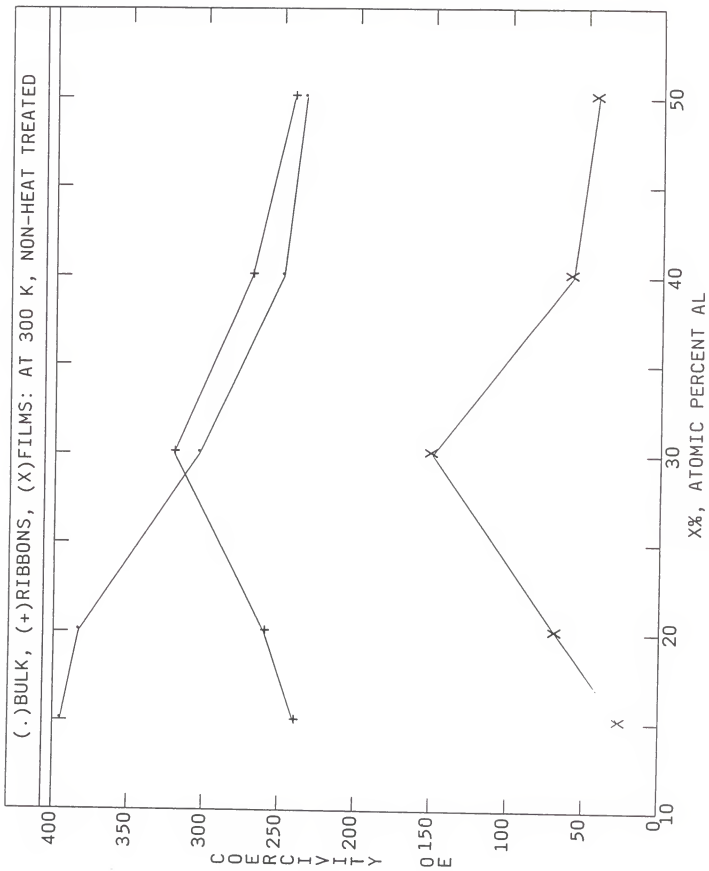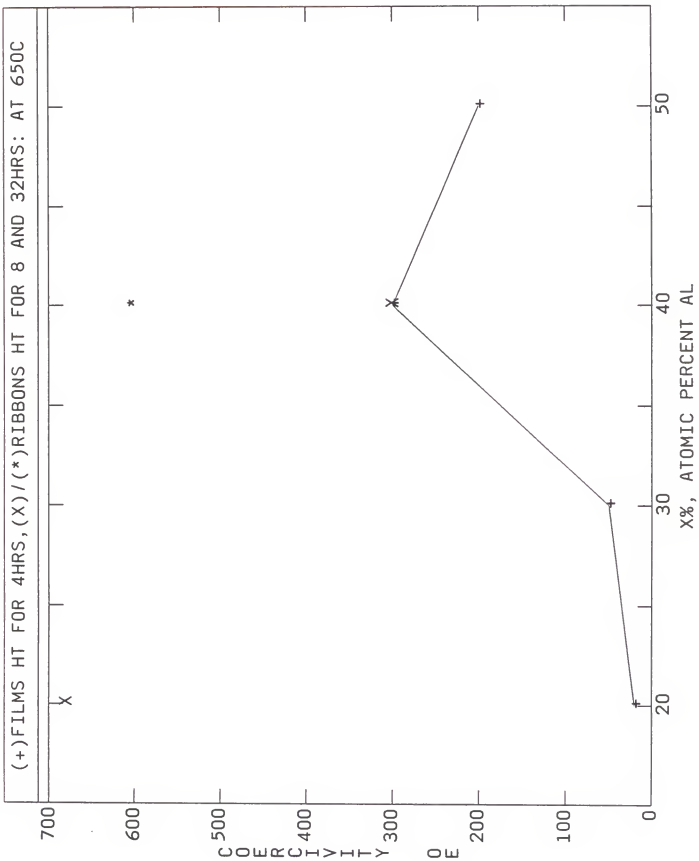
CONDUCTIVITY

OE

X%, ATOMIC PERCENT AL

Figure 3.3 : Coercive fields of heat treated Co-Al alloys; thin films, and ribbons.

(+)FILMS HT FOR 4HRS, (X)/(*)RIBBONS HT FOR 8 AND 32HRS: AT 650C

X%, ATOMIC PERCENT AL

COERCIVITY OE

21a

Heat treatment of ribbons also leads to increased coercivities. However, heat treatment at very high temperatures, i.e. 850^0 C for 4 hours, results in reduction of the coercivity due to the excess precipitation of Co-rich particles. This is illustrated in Figure 3.4 for $Co_{70}Al_{30}$. The same behavior has been observed for all the films that were heat treated to 850^0 C for the same time intervals.

The maximum magnetic hardening of Co-Al ribbons of different compositions was obtained by heat treating for various time intervals. The resulting coercivities are plotted as a function of the time of heat treatment in Figure 3.5 for $Co_{80}Al_{20}$ and $Co_{60}Al_{40}$ ribbons. It is observed here that the heating time required for obtaining maximum coercivity varies with the composition. That is, the optimum coercivity for the $Co_{80}Al_{20}$ was obtained after heat treating the specimens for 8 hours, and this final value for coercivity was about 679 Oe. Similarly, the rest of the alloys were heat treated for optimizing time intervals in order to attain their peak magnetic hardening (fig. 3.5). The different heating times required for each composition result from the varying Co content in each of them. This means that the larger the amount of Co present in the heat treated alloy the faster the Co-rich phase precipitation will occur and consequently the smaller the heat treatment time required.

3.1.2 The magnetization of thin films, ribbons,and bulk $Co_{100-x}Al_x$ alloys

The saturation magnetization, M_s, was measured for as-deposited and heat treated thin films, ribbons, and bulk specimens of Co-Al. The values of saturation magnetization were found to be larger for thin films than those for bulk and ribbon alloys. This is again due to the different microstructure observed in the various forms of the Co-Al alloys. It should be noted, however, that the values of saturation magnetization for the films are significantly reduced by heat treatment.

Figure 3.4 : Hysteresis loops of as-deposited and heat treated (850^0C, 4hrs) $Co_{70}Al_{30}$ thin films.
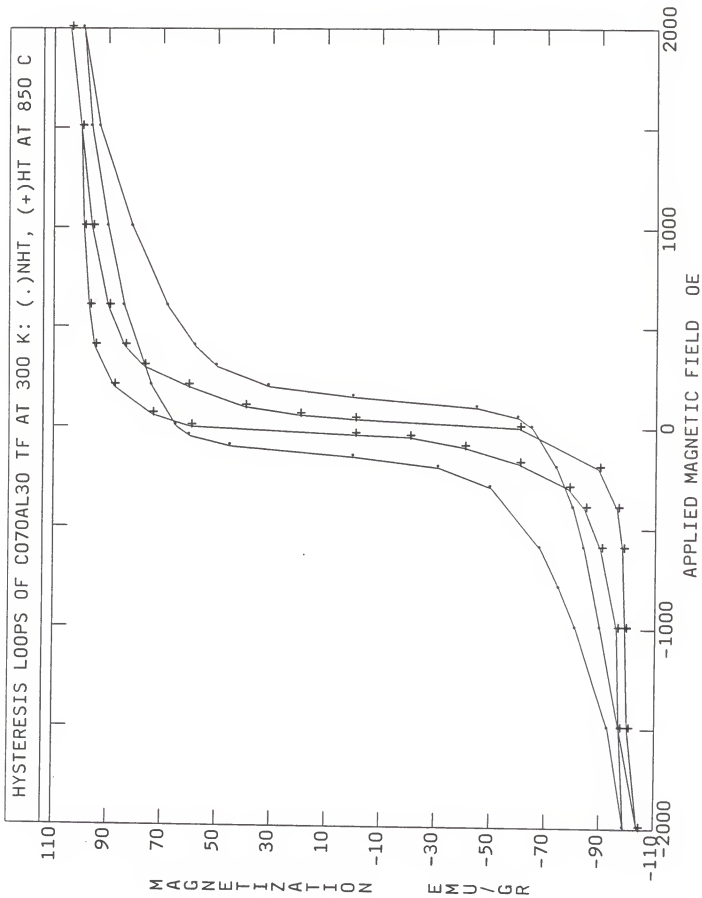
HYSTERESIS LOOPS OF CO70AL30 TF AT 300 K: (.)NHT, (+)HT AT 850 C

APPLIED MAGNETIC FIELD OE

MAGNETIZATION EMU/GR

23a

Figure 3.5 : Coercive fields as a function of heat treatment times for Co-Al ribbons.

COERCIVITY VS. TIME OF HEATING : (+)CO80AL20, (*)CO60AL40

HEATING TIME HRS.

COERCIVITY OE

24a
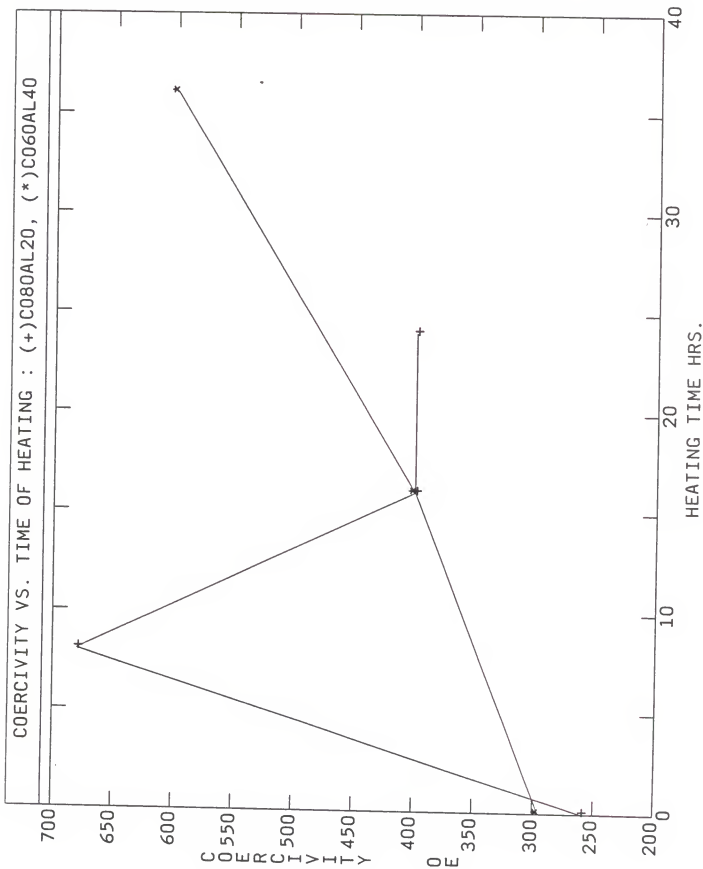
Figure 3.6 shows the saturation magnetization plotted as a function of chemical composition for as deposited thin films, and as cast bulk and ribbon alloys. The values obtained for the saturation magnetization of the heat treated specimens of the Co-Al alloys are shown in Figure 3.7. The values of saturation magnetization are still found to be larger than those for bulk and ribbons of the same chemical composition. This observation reinforces the idea of different microstructure in the studied forms of Co-Al alloys. The study of bulk alloys was not pursued further since there is already an abundance of information on this subject in literature.

3.1.3 Thermomagnetic data for thin film, and ribbon $Co_{100-x}Al_x$ alloys

Thermomagnetic measurements for as deposited thin film samples were obtained for the various compositions of $Co_{100-x}Al_x$. The change in the magnetization of the films as a function of temperature was monitored up to about 700^0 C in order to observe the phase transitions in the specimen as the temperature changed and to obtain the crystallization or Curie temperature of the specific chemical composition . Figure 3.8 shows magnetization as a function of temperature for $Co_{80}Al_{20}$ thin films. This figure indicates the value of the Curie temperature for the bcc-CoAl phase, which has a numerical value of about 160^0 C. The other transition, which occurs at about 500^0 C, is attributed to the Co_3Al phase that is present in the heat treated films as indicated by their electron diffraction patterns. In Figure 3.9 the magnetization as a function of temperature is presented for $Co_{60}Al_{40}$ thin films. Three transitions are observed for this composition also, occuring at around 160^0 C, 200^0 C and 500^0 C. The magnetic transition temperature at 160^0 C is considered to be the Curie temperature of the CoAl-bcc phase present in this type of as deposited films. The higher temperature transitions are believed to correspond to the hcp-Co $(200^0$ C), and the Co_3Al $(500^0$ C), phases resulting in the heat treated thin films.

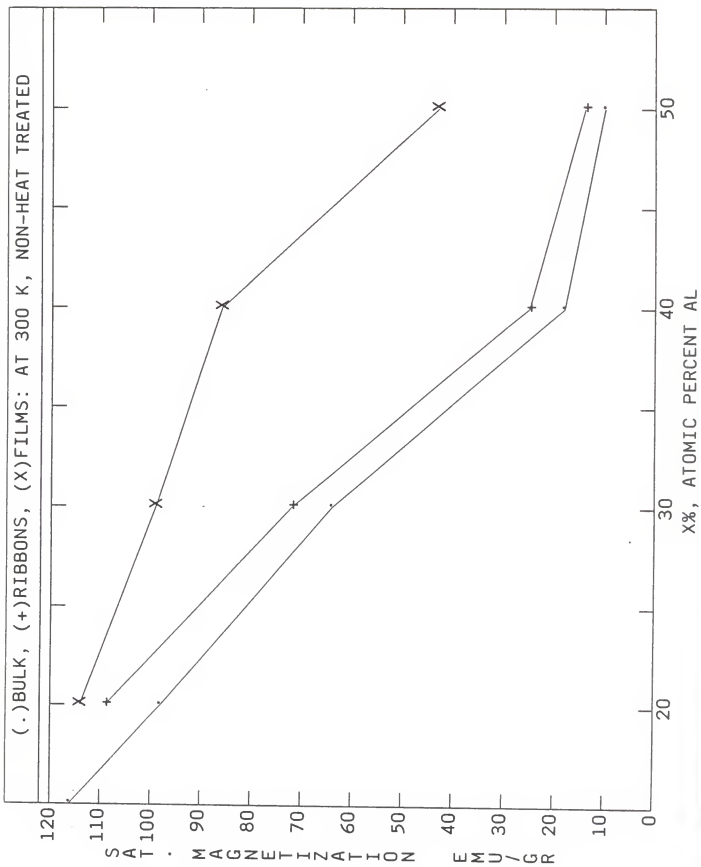Figure 3.6 : Magnetization as a function of chemical composition in non-heat treated Co-Al alloys.

(.)BULK, (+)RIBBONS, (X)FILMS: AT 300 K, NON-HEAT TREATED

STATE MAGNETIZATION EMU/GR vs. X%, ATOMIC PERCENT AL

26a

Figure 3.7 : Magnetization as a function of chemical composition in heat treated Co-Al alloys.

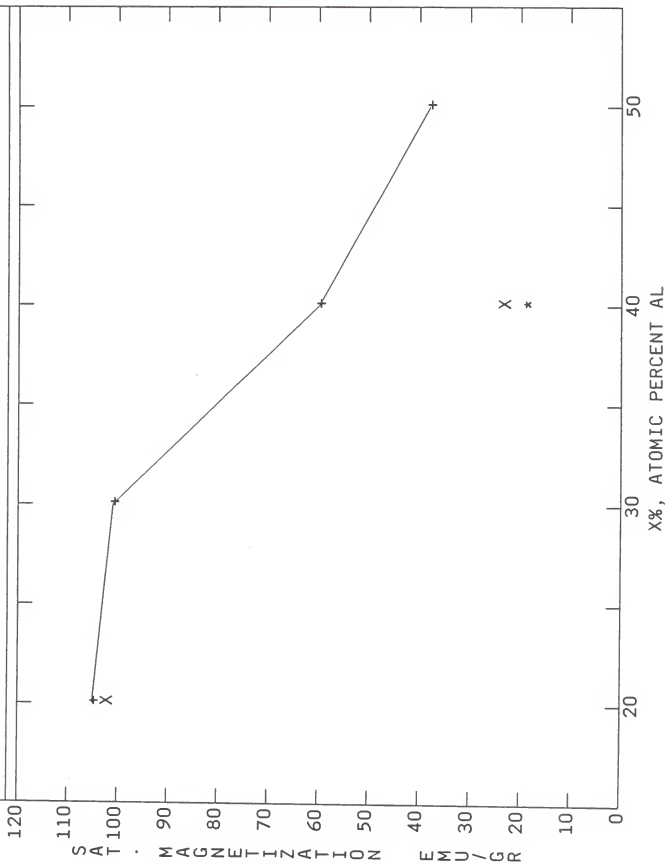(+)FILMS HT FOR 4HRS, (X)/(*)RIBBONS HT FOR 8 AND 32HRS: AT 650C

X%, ATOMIC PERCENT AL

STAT. MAGNETIZATION EMU/GR

27a

Figure 3.8 : Thermomagnetic data for $Co_{80}Al_{20}$ thin films.

THERMOMAGNETIC DATA OF CO80AL20 FILMS: H(APPLIED)=800 OE

28a
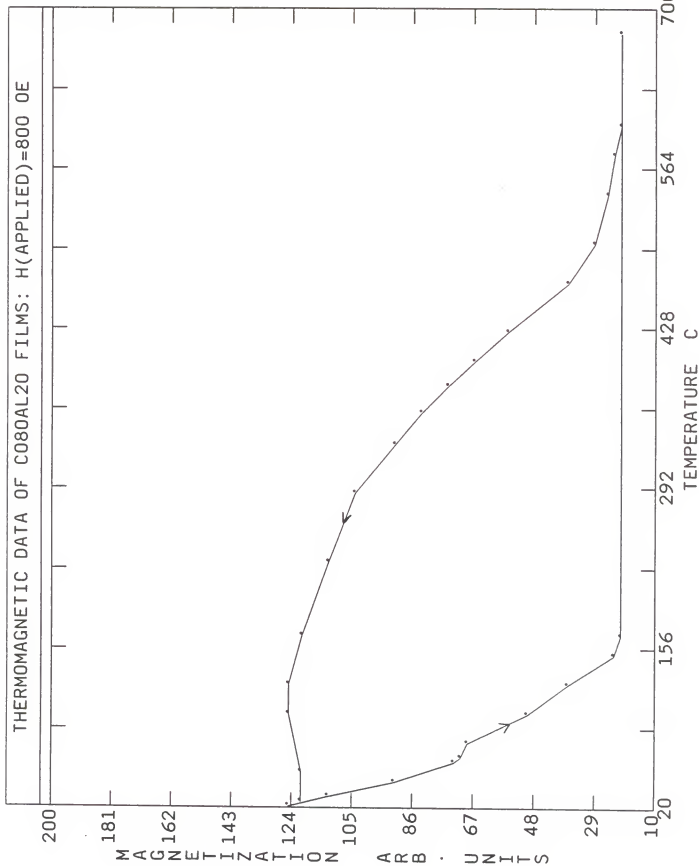
Figure 3.9 : Thermomagnetic data for $Co_{60}Al_{40}$ thin films.

THERMOMAGNETIC DATA OF CO60AL40 THIN FILMS: H(APPLIED)=800 OE

29a
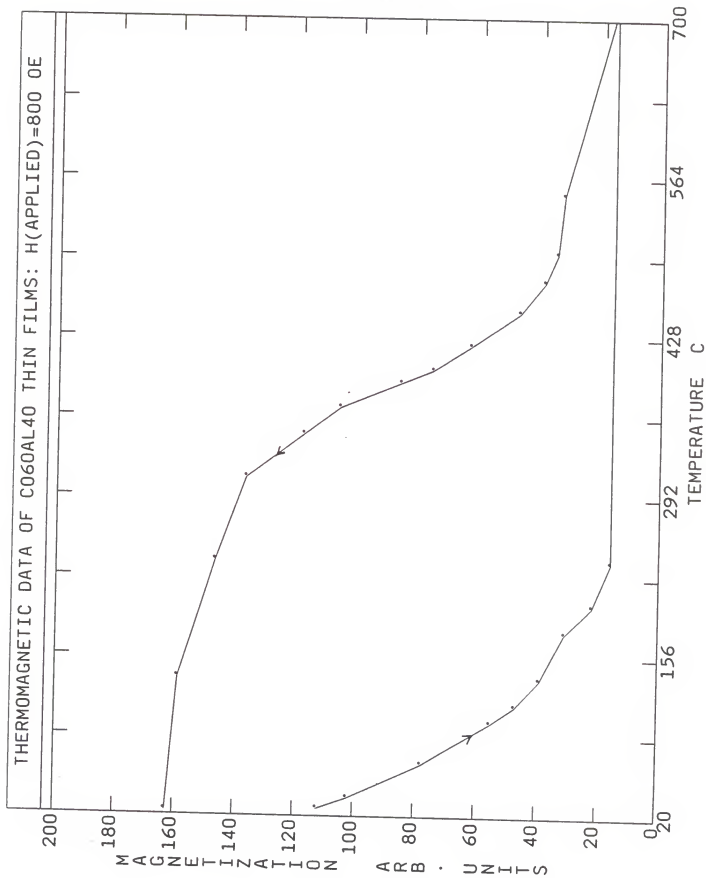
Figure 3.10 : Thermomagnetic data for $Co_{80}Al_{20}$ ribbons.

THERMOMAGNETIC DATA OF CO80AL20 RIBBONS : H=800 OE

30a
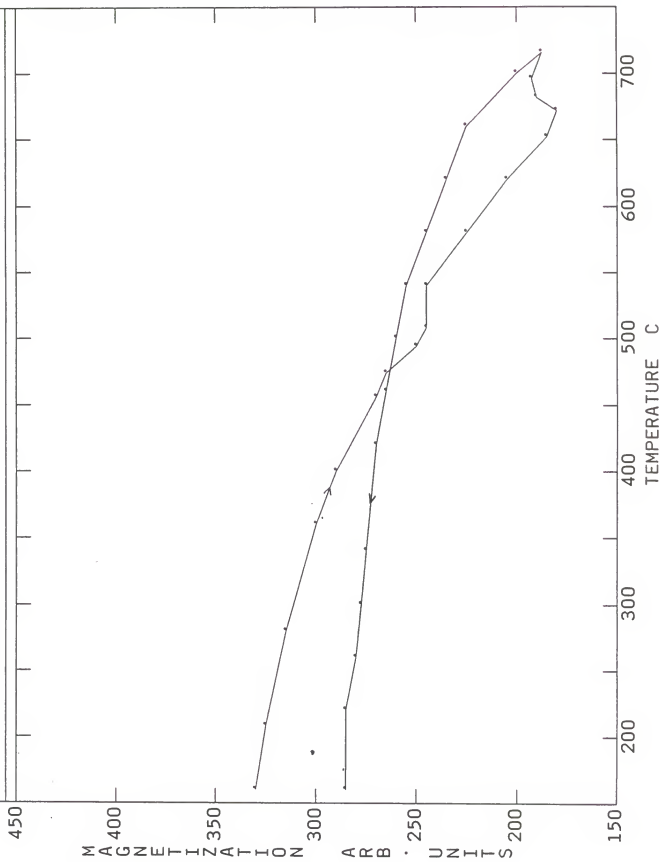
Thermomagnetic information was also obtained for ribbons of the various chemical compositions studied. In Figure 3.10 the variation of magnetization in $Co_{80}Al_{20}$ ribbons is shown as a function of temperature. Two magnetic transitions are observed, one at 510^0 C and another at 675^0 C. These cannot be the only transitions present however, since the magnetization is found to be well above zero for both transitions even after subtracting the background signal. It is believed that such a transition will originate from Co-rich particles since for pure Co the characteristic Curie temperature is equal to 1131^0 C [5]. The lower temperatures recorded, however, indicate two phase transitions that can be explained as follows: The transition occuring at 510^0 C is probably an fcc-Co_3Al transition, while the one occuring at 675^0 C is also a Co-rich transition. Figure 3.11 shows the thermomagnetic information obtained for $Co_{60}Al_{40}$ ribbons. The transition observed at 160^0 C may be due to the presence of a bcc -CoAl phase.

Ac susceptibility measurements of as deposited films in the temperature range of 297 K to about 4.2 K did not show any significant structure changes in the temperature range studied, with the exception of the $Co_{60}Al_{40}$ films for which a quite transition occurs at approximately 90 K (Figure 3.12). The origin of this transition is not clear from these results. Ac susceptibility measurements of the Co-Al ribbons gave no significant information regarding the magnetic behavior of the alloys below room temperature . An exception should be made for the $Co_{60}Al_{40}$ ribbons which undergo a similar phase transition at about 100^0 K. It should also be noted that heat treated ribbons of the Co-Al alloys do indicate the magnetic hardening that results from the heat treatment, when Ac susceptibility measurements are obtained. In these samples magnetic phase transitions are found to occur in the range of $(100-200)^0$ K, depending on the chemical composition of the sample.

Figure 3.11 : Thermomagnetic data for $Co_{60}Al_{40}$ ribbons.

THERMOMAGNETIC DATA OF CO60AL40 RIBBONS : H=800 OE

32a

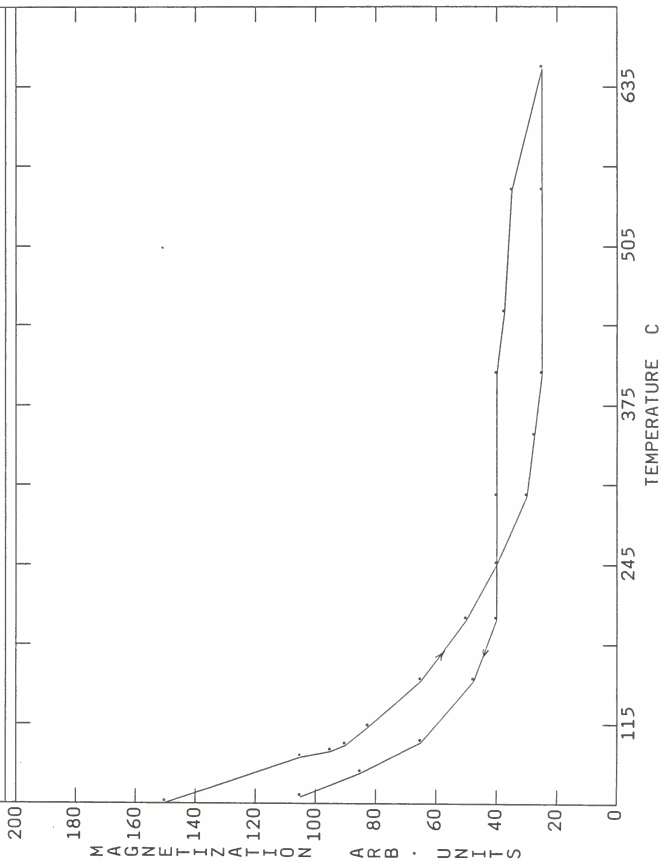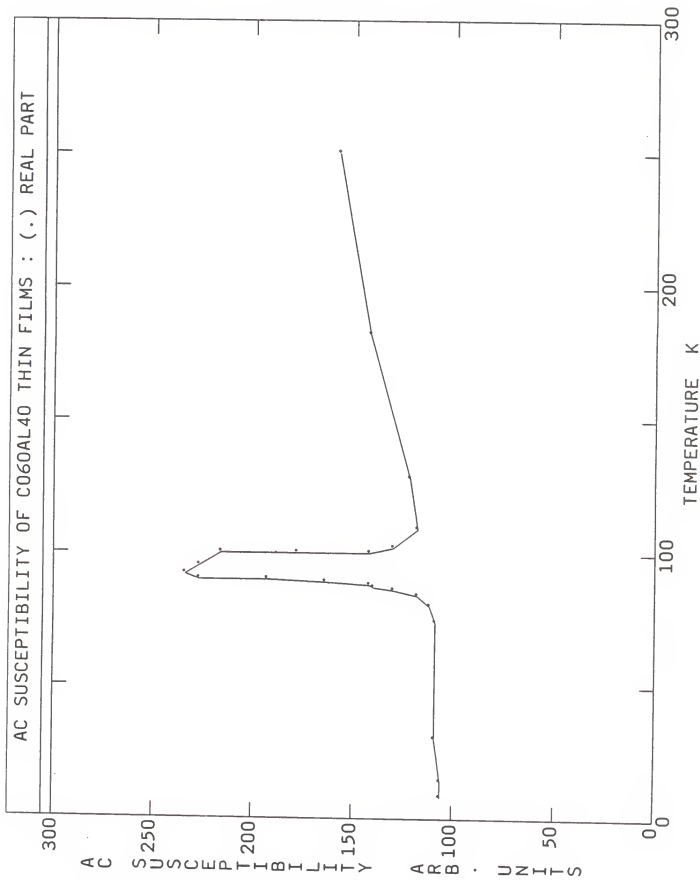Figure 3.12 : Ac susceptibility data for as-deposited $Co_{60}Al_{40}$ thin films.

AC SUSCEPTIBILITY OF CO60AL40 THIN FILMS : (.) REAL PART

ACSUSCEPTIBILITY ARB. UNITS

TEMPERATURE K

33a

3.2 Microstructure

3.2.1 Properties of $Co_{100-x}Al_x$ thin films

$Co_{100-x}Al_x$, with $20 \leq x \leq 50$, thin films were studied in terms of their crystal structure in order to obtain a further insight in their magnetic behavior. Electron diffraction patterns of films with $x \leq 25$ showed strong Debye rings of the hcp-Co phase which is the dominant phase recorded. However, there must be an fcc-Al phase present, because of the Al content indicated by the chemical composition analysis. If present, its presence is masked by the strong hcp-Co reflections. Figure 3.13a shows a diffraction pattern for $Co_{80}Al_{20}$ thin films, which is characteristic for compositions with $x \leq 25$. Brightfield pictures of the crystal microstructure indicate a grain size of about 100 A (Figure 3.14a). Figure 3.14a also shows the fine microstructure of the Co-Al thin films, which is characteristic for differentiating between the thin films and the bulk and ribbon alloys of the same composition. Figue 3.15a shows the magnetic domain structure of the $Co_{80}Al_{20}$ thin films. The clear domain walls and strong ripples of magnetization observed here, are characteristic of the thin films with aluminium content $x \leq 25$.

When the aluminum content of the as deposited films is increased above 25% atomic the resulting crystal structures were found to be cubic. Specifically, for x=30 the cubic phase corresponded to disordered bcc-CoAl. As the aluminum content was increased (i.e., x=40, x=50) partially ordered bcc-CoAl structures were obtained as indicated by weak superlattice reflections in their diffraction patterns. Figure 3.16a shows the diffraction pattern obtained for $Co_{70}Al_{30}$ thin films, corresponding to the disordered bcc-CoAl phase. Figure 3.17a presents the microstructure of $Co_{70}Al_{30}$ thin films and indicates a grain size of about 150 A. The domain structure of these films is characterized by fine ripples of magnetization. It is also noted that there are no domain walls which indicates the presence of an anisotropy with a pronounced perpendicular component (fig. 3.18a).

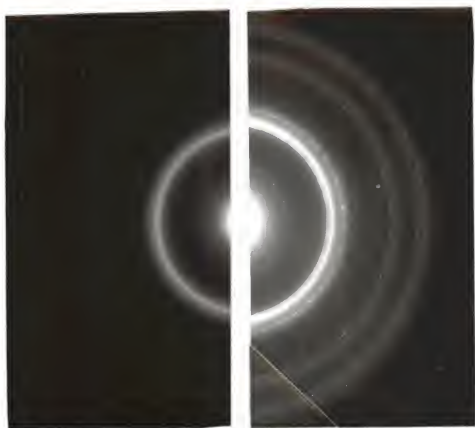It was mentioned earlier that thin films with aluminum content with

Relative magnifications for the microstructure and
domain pictures

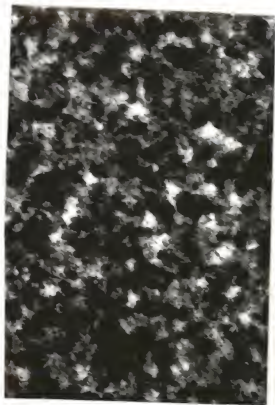Figure 3.13 : Electron diffraction pattern of as deposited (a), and heat treated (b) $Co_{80}Al_{20}$ thin films.

a   b

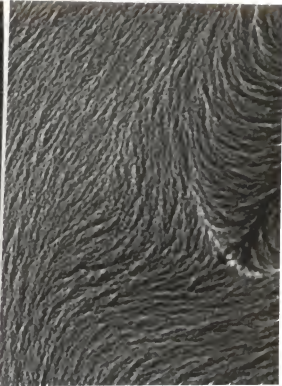Figure 3.14 : Microstructure of as-deposited (a), and heat treated (b) $Co_{80}Al_{20}$ thin films.

a

b

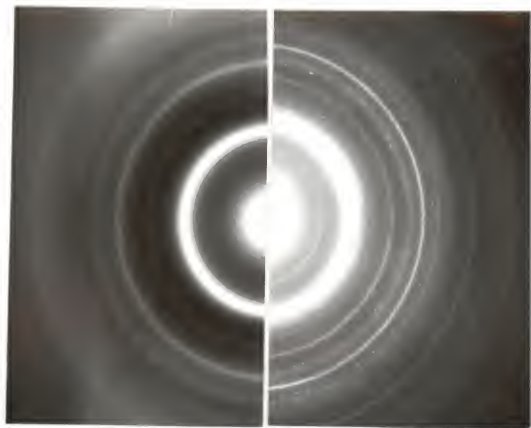Figure 3.15 : Magnetic domain structure of as-deposited (a), and heat treated (b) $Co_{80}Al_{20}$ thin films.

a   b

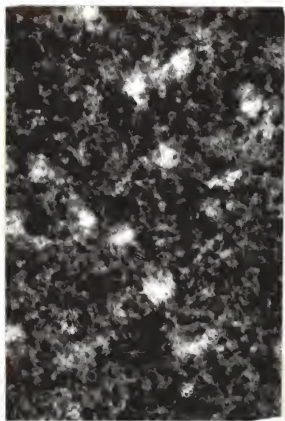Figure 3.16 : Electron diffraction pattern of as-deposited (a), and heat treated (b) $Co_{70}Al_{30}$ thin films.

a   b

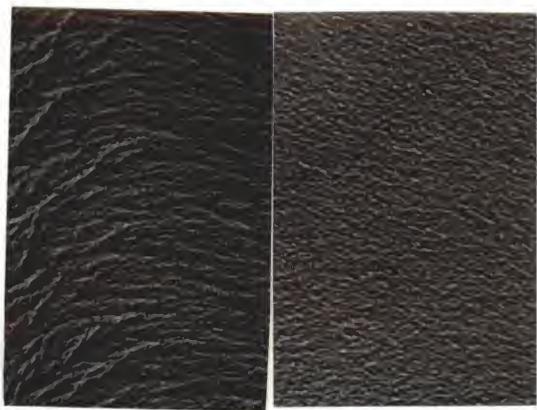Figure 3.17 : Microstructure of as-deposited (a), and heat treated (b) $Co_{70}Al_{30}$ thin films.

a   b

Figure 3.18 : Magnetic domain structure of as-deposited (a), and heat treated (b) $Co_{70}Al_{30}$ thin films.

a   b

$x \geq 30$ have a partially ordered bcc-CoAl structure. Figure 3.19a and 3.20a show the diffraction patterns, the microstructure, and the magnetic domain structure for the thin films of aluminium content x=40 and x=50 respectively. The former have grains whose size varies between (100-200)A and fine magnetic domain structure, while the latter have small grains (50 to 100 A) and very weak domain structures.

The structure of the films is drastically changed after heat treating at 650^0 C for 4 hours. Figure 3.13b exhibits the diffraction pattern obtained for heat treated $Co_{80}Al_{20}$ thin films, that is characteristic for heat treated thin films of aluminium content with $x \leq 25$. The resulting crystal structure indicated by this diffraction pattern is a mixture of hcp-Co with a phase that is interpreted as ordered fcc-Co_3Al. The calculated lattice constant for the fcc-Co_3Al phase is $\alpha = 3.568$ A [31] . The fine microstructure shown in Figure 3.14b indicates hcp -Co of grain size that is about 100 A. The magnetic domain structure (figure 3.15b) indicates finer ripples of magnetization without domain walls, that is again an indication of anisotropy with a pronounced perpendicular component.

Heat treated films with aluminum content of $x \geq 25$ contain the following two phases: fcc-Co_3Al and bcc- CoAl . $Co_{70}Al_{30}$ heat treated films are shown in figures 3.16b, 3.17b, and 3.18b. The diffraction patterns obtained for this composition are a mixture of fcc-Co_3Al and bcc-CoAl phases. The grain size of the latter is about 200 A while the grains of the former are widely separated and vary between 200 A and 800 A. The magnetic domains appear to be coarsened with a less pronounced perpendicular component after the heat treatment.

Figures 3.19b and 3.20b show the crystal structure of heat treated thin films with aluminum content of $x \geq 30$. $Co_{60}Al_{40}$ heat treated thin films consist of the fcc-Co_3Al and the bcc-CoAl phases. The grain size of the Co_3Al phase varies between 400 A and 500 A, and that of bcc-CoAl phase is about 200 A. The domain structure of the heat treated $Co_{60}Al_{40}$ films indicates a coarsening in the structure of the domains and a less pronounced perpendicular component. The changes

41

Figure 3.19 : The diffraction patterns, the microstructure, and the domain structure of as-deposited (a) and heat treated (b), $Co_{60}Al_{40}$ thin films.
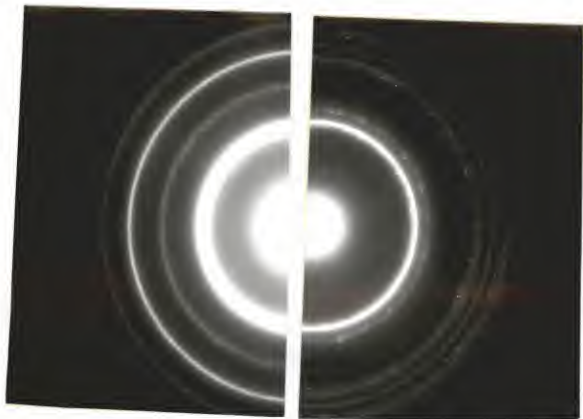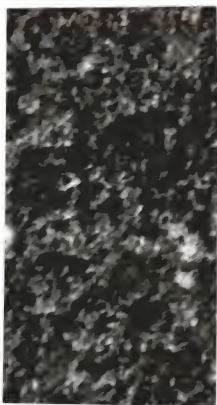
a   b
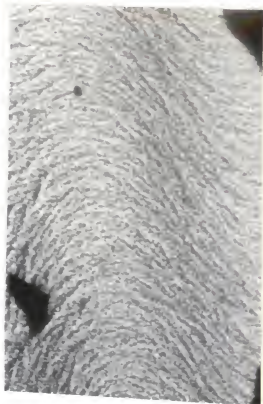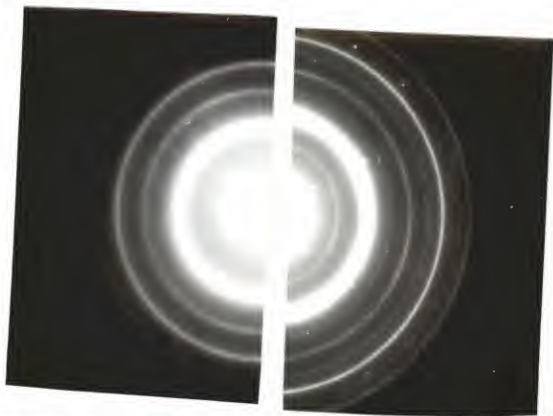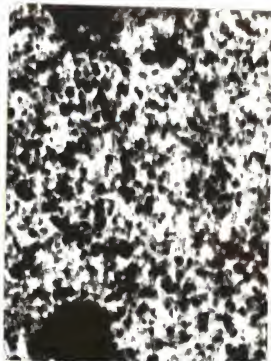
Figure 3.20 : The diffraction pattern, the microstructure, and the domain structure of as-deposited (a) and heat treated (b), $Co_{50}Al_{50}$ thin films.

a   b

43a

observed in the diffraction pattern of heat treated $Co_{50}Al_{50}$ films indicate an ordered bcc- CoAl phase along with strong Co_3Al reflections. The grain sizes of the former vary between 100 A and 200 A, while those of the latter range from 1000 A to 1100 A. The domain structure exhibits further coarsening and there is no specific orientation of the anisotropy components.

3.2.2 Properties of $Co_{100-x}Al_x$ bulk and ribbon alloys

It was mentioned earlier that bulk specimens of Co-Al, with various Al contents, had their properties thoroughly examined in the past and the results of the works of H. Masumoto et al. [15], A. Zeltser et al. [10], K. Masui et al. [14], and R. Jonhson et al. [9] constitute a complete account on the subject.

The diffraction patterns of the $Co_{100-x}Al_x$ ribbons with $x \leq 25$ indicated a mixture of phases. The precipitated phase was mostly hcp-Co. The calculation of the interplanar spacings indicates the presence of another phase which has not been identified but is believed to cause the lamellar structure seen in the ribbons (figure 3.22b). The irregularities in the ribbon formation have among other things helped in the development of the lamellar structure which involves regions of opposing magnetic moments. This is deduced from the different orientations of the elongated particles (grains) present in each of the parallel sections of the lamellar structure (as per fig. 3.22b). Figure 3.21 shows the diffraction pattern obtained for $Co_{80}Al_{20}$ ribbons. The microstructure of these ribbons indicates the complicated nature of these materials as well as the large size of their precipitates (figure 3.22a). The grain size is shown considerably larger than that of thin films and in general the microstructure is very different than that seen in films. As the aluminum content increases the crystal structure is changed, but we still encounter the Co rich phases. For $x \geq 25$ the precipitated phases are mostly Co-rich phases of hcp Co and fcc Co (figure 3.23). The microstucture is also very different from that encountered in thin films of similar chemical compositions (figure 3.24).

Figure 3.21 : Diffraction patterns of as melt-spun $Co_{80}Al_{20}$ ribbons.

45a

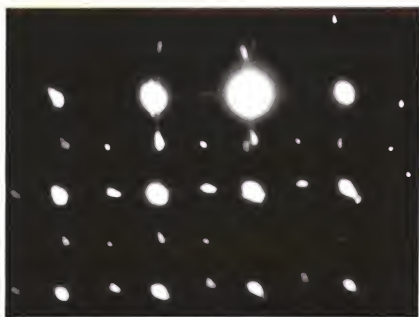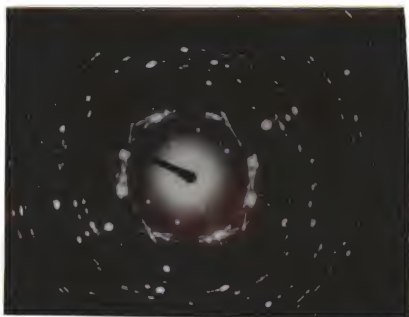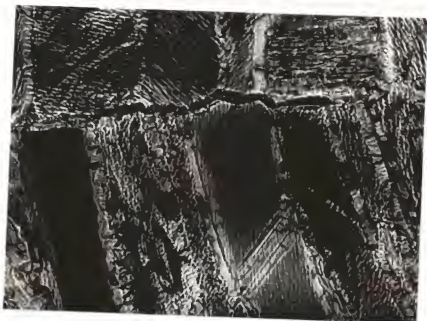Figure 3.22 : Microstructure of as melt-spun (a,b), and heat treated (c,d) $Co_{80}Al_{20}$ ribbons.

a

b

46a
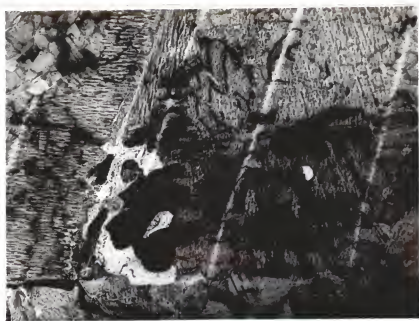
c

d

Figure 3.23 : The diffraction pattern of as melt-spun $Co_{60}Al_{40}$ ribbons.
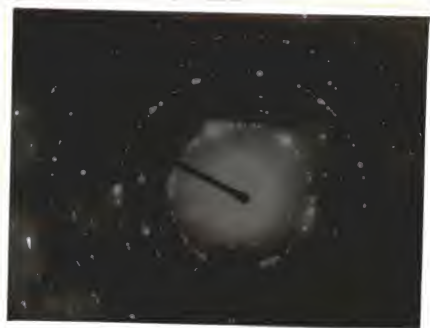
Figure 3.24 : The microstructure of as melt-spun $Co_{60}Al_{40}$ ribbons.

Co-Al ribbons were also heat treated in order to obtain the maximum magnetic hardening for each of the chemical compositions. Ribbons with aluminum content of $x \leq 25$ required heating times of about 8 hours to optimize their magnetic properties. The diffraction patterns obtained for the heat treated ribbons and their respective X rays indicate the presence of hcp Co particles along with weak reflections of Co_3Al. This indicates a further precipitation of the Co rich phases that causes the measured increase in the coercivity. Figure 3.25 shows the diffraction pattern obtained for heat treated $Co_{80}Al_{20}$ ribbons. The microstructure of the same ribbons indicates larger grains and a coarser lamellar structure reinforced by the unidentified phase (figure 3.22 c,d). This phase may be linked with the hybrid Sato phase discussed by Zeltser [10] (figure 3.25).

Heat treated ribbons with $x \geq 25$ show further precipitation of Co rich phases, that is, hcp Co and fcc Co along with some stronger reflections of the Co_3Al phase as it is indicated by the X-rays obtained for the heat treated Co-Al ribbons with $x \geq 25$. Figure 3.26 shows the diffraction pattern obtained for $Co_{60}Al_{40}$ ribbons and from which the phase calculations were obtained. The microstructure of these ribbons (x=40) indicates a considerable change after heat treating for 32 hours. In figure 3.27 the microstructure is shown, for the $Co_{60}Al_{40}$ ribbons, which indicates a large grain size and it cannot be considered as comparable to the respective microstructures obtained for thin films of similar compositions.

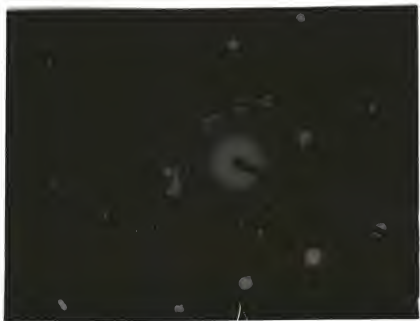Figure 3.25 :The diffraction pattern of heat treated $Co_{80}Al_{20}$ ribbons.

50a

Figure 3.26 : The diffraction patterns of heat treated $Co_{60}Al_{40}$ ribbons.
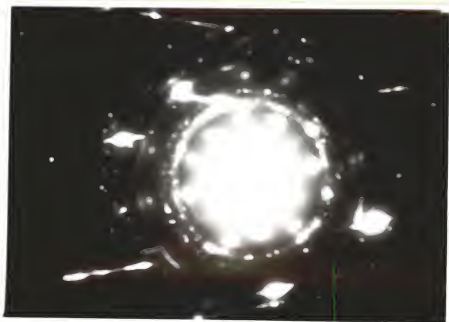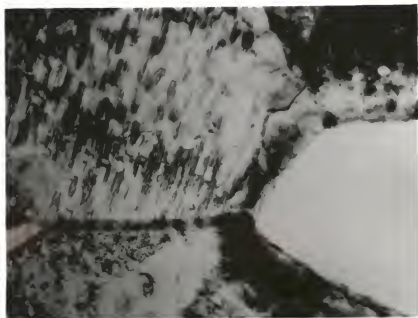
Figure 3.27 : The microstructure of heat treated $Co_{60}Al_{40}$ ribbons.

4. DISCUSSION

4.1 Assessment of the crystal structure of $Co_{100-x}Al_x$ alloys

The structure of thin films prepared by vacuum evaporation depends on factors such as the rate of deposition, the pressure during deposition, the nature of the substrate, etc. as it was mentioned earlier. The Co-Al thin films were all prepared under the same conditions so that their resulting structure would be a strong function of chemical composition . The structural investigation indicates that there is a Co-rich phase present in the high Co content films while a magnetic bcc-CoAl phase is present in the lower Co content films. Heat treatment of the films results into the precipitation of another Co-rich phase, that is Co_3Al, in all of the thin films, which causes an increase in their coercivity as mentioned earlier. The Co_3Al phase found in all the heat treated films is possibly a metastable phase; that could explain why it is not found in the stable phase diagrams of Co-Al alloys [12,14].

The domain walls observed in these films are characterized as Bloch walls, since the film thicknesses were in the 1000 A range . Neel walls are not very plausible in these materials since the maximum film thickness for Neel walls to occur is about 300 A. The magnetic domains in the Co-Al thin films showed magnetization ripples. Magnetization ripples occur because the magnetization, M_s, varies in a wave like manner in order to minimize the exchange and magnetostatic energies [5,6,7,8].

The Co-Al ribbons studied in this project have exhibited a mixture of phases, the most prominent of which were those of fcc-Co and hcp-Co. After heat treatment, a precipitation took place and this led to an increase in coercivity. The magnetic domain structure and microstructure were mostly complicated as would be expected from the multitude of the phases present.

Furthermore, the Co-Al ribbons studied, exhibited a radically different structure morphology than the thin films of similar compositions. The microstructure

studies in the ribbons showed that they are not as uniformly structured as the thin films of Co-Al. This was made evident from the different morphologies obtained from the different areas of the ribbons studied. The reason for the development of such structural irregularities in the ribbons is that the chemical compositions chosen for these studies are not close to a deep eutectic point so that they can form a glass like matrix when prepared by melt-spinning, as it has been discussed earlier (chap.1;section 1.2).

The electron microscopy studies of the Co-Al ribbons have indicated a very complicated crystal structure which was very difficult to decompose into its single phase constituents by using a low intensity, point like electron beam technique, that is usually employed for these studies[23,24,25]. It was mentioned earlier that there were a few strong single phases that could be singled out and characterized as hcp-Co and fcc-Co, but in depth analysis of these ribbons in terms of their crystallographic behavior, and subsequently of their magnetic behavior with respect to the magnetic phases present, remains to be completed.

4.2 Assessment of the magnetic behavior of $Co_{100-x}Al_x$ alloys

The magnetic behavior of bulk Co-Al alloys has been already discussed in the literature [9,10,11,12,13,14,15]. It has been reported that heat treated bulk samples of Co-Al alloys have an increased value in coercivity, which has been attributed to the precipitation of Co particles into a CoAl matrix. The precipitates are said to be single domain particles according to electron diffraction studies and this property can be used to explain the high coercivities and the classification of such materials as hard magnetic materials.

Thin films, just as bulk materials, are expected to exhibit structure dependent and structure independent properties. Structure dependent properties of thin

films and bulk alloys, are such quantities as the coercivity and in general their magnetic hysteresis. The Curie temperature of the various Co-Al magnetic phases, and their saturation magnetization are intrinsic properties, which are characteristic of the phases present. It should be noted that the M_s values of thin films of similar chemical compositions were reproducible without any discrepancies. However, the saturation magnetization of the Co-Al thin films was found to be different from the saturation magnetization values measured for the Co-Al bulk alloys of the same chemical composition. Such a behavior may be attributed to the difference in the microstructure of the samples studied. The microstructure of the samples consisted of multiple phases. This leads to the assumption that the magnetization values observed are the average of the magnetizations of all the phases present. Furthermore, the microstructure of the samples varies with composition and heat treatment, which is the reason for the differences observed in the results. In bulk alloys the rate of cooling during the preparation of the samples is much different than that in films, and therefore, the microstructure and the subsequent measured values of magnetization are different. In addition, the recorded decrease in the magnetization with increasing aluminum content, is attributed to the increase in the amount of Co_3Al and Co-Al phases which are less magnetic than the Co phase. Furthermore, the heat treatment of the thin films caused their saturation magnetization to decrease. This decrease can be explained by the change in the composition of the precipitate and the magnetic matrix.

It was mentioned earlier (chap1) that the magnetization of thin films is reversed by domain wall motion in the lower applied fields and by rotation of the magnetization at the higher fields, which can be in coherent or in incoherent mode. The magnetization reversal by Stoner-Wohlfarth coherent rotation has been found to occur when the ratio of the remanent magnetization, M_r, to the saturation magnetization, M_s, is about 0.5 for uniaxial materials. The values of M_r/M_s for the thin films of various chemical compositions were calculated in the range of 0.6 to 0.8. This deviation can be attributed to the magnetic behavior of the bcc-CoAl matrix. It was observed that the deviation increased with Co content, that is for

x=50 the magnetization ratio value was equal to 0.6, while for x=80, the other extreme of the compositions studied, the magnetization ratio value was equal to 0.78. The increase in the coercivity values of the heat treated thin films is attributed to the precipitation of the Co_3Al crystallites in the bcc-CoAl matrix leading to a fine microstructure that possibly causes domain wall pinning. This is evidenced by the Lorentz microscopy studies which clearly showed the presence of domain walls.

The Co-Al alloys in ribbon form, were found to exhibit relatively high coercivity values after appropriate heat treatment. This magnetic behavior has been studied and correlated with the results reported in literature. H.Masumoto et al.[15], R. Johnson et al.[9], and A. Zeltser et al.[10], have attributed a similar behavior in bulk alloys to the precipitation of Co-rich single domain particles in association with a non-magnetic CoAl matrix. Zeltser and Masumoto concluded that the difficulty to rotate the magnetzation that is caused by the opposing large energies of crystal and shape anisotropy in the single domain particles. Johnson, however, attributes this behavior to the influence of the magnetic matrix present which causes the suppression of coercivity. Thus the specimen needs to undergo heat treatment for the precipitation to occur and cause the matrix to become non-magnetic, and the coercivity to increase. The results obtained in this project, for the Co-Al ribbons, do not support either of the previous arguments, since they exhibit a very different microstructure than that reported in the literature.

The chemical composition analysis of the small areas selected for phase characterization studies, has indicated a large variation in the relative amounts of Co and Al present. This is an additional confirmation of the non- eutectic nature of the chemical compositions studied. The relatively high coercivities exhibited by these alloys are possibly related to this complicated microstructure and specially to the presence of the thin lamellae. The interactions of the domain walls with all these microstructural features needs to be determined.

5. CONCLUSIONS

The work presented in this report was undertaken in an effort to study the differences between bulk alloys and thin films of Co-Al of similar chemical compositions, and further to determine whether thin films of Co-Al can be considered as good candidates in memory devices applications.

The properties of thin films studied, have proven them to be soft magnetic materials in contrast with their bulk counterparts which when subject to heat treatment become relatively hard magnetic materials. This magnetic behavior renders thin films of Co-Al not the ideal candidate for magnetic recording. The study of the crystal structure of thin films of Co-Al and that of bulk alloys of similar chemical compositions have shown characteristic differences between these two types of Co-Al alloys. That is, there seems to be a different phase distribution in each of them, with films being able to exhibit metastable phases as a permanent feature which is not characteristic of the bulk materials. The presence of the Co_3Al phase in the ribbons is possibly due to the fact that ribbons are in a state with a structure that lies in between the bulk and thin film texture. The differences in the respective structures of thin films and bulk materials can be considered as the major factor that causes their magnetic behavior to be different.

It should also be pointed out that the melt-spun ribbons of the Co-Al alloys exhibited a complicated structure which was rather different from that reported in the literature [9,10,11,12,13,14,15] for bulk alloys of Co-Al. However, this difference in the structure did not affect the magnetic behavior of the ribbons, which upon heat treatment exhibited relatively high coercivities. These studies on Co-Al thin films have contributed to a further understanding of the thin films mechanisms in general. The work involved in the preparation and study of these films has enabled the author to pinpoint several factors that contribute in the manufacture of better

quality films. A better understanding of the theoretical models involved in the explanation of the magnetic hysteresis behavior of films was also possible.

Finally it should be noted that the field of thin film study is quite complex and has yet to be clarified further before definite answers are obtained for their structural and magnetic behavior[26,27,28,29,30,32]. In conclusion, one should note the following regarding the complexity of evaporated thin films as it is very well conceived by Pugh [5] when he discusses " the metallurgical nightmare of imperfections, impurities, and stresses, which externally appear as shiny thin films".

REFERENCES

1 . L. Holland, Vacuum deposition of thin films, J.Wiley and sons Inc., (1965)

2 . O.S. Heavens, Thin Films Physics, London, (1970)

3 . R. Zallen, The physics of amorphous solids, J.Wiley and sons, (1983)

4 . S.R. Elliot, Physics of amorphous materials, Longman, (1952)

5 . B.D. Cullity, Introduction to magnetic materials, Adisson-Wessley, (1972)

6 . A.H. Morrish, The physical principles of magnetism, J.Wiley and sons Inc., (1965)

7 . G.T. Rado, H. Suhl, Magnetism vo.3, Academic press, pp. 415-, (1963)

8 . J. Crangle, The magnetic properties of solids, E. Arnold, pp.110- , (1977)

9 . R.E. Johnson, H.W. Rayson,and W. Wright, Acta Met.,20, 387, (1972)

10 . A.M. Zeltser and W.A. Soffa, IEEE Trans. Magn.,MAG-22, 588, (1986)

11 . H.L. Luo and P. Duwez, Can. J. Phys., 41, 758, (1963)

12 . A.J. Bradley, G.C. Seager, J. Inst. Metals, 39, 81, (1964)

13 . M.P. Arbutov, A.A. Pavlyukov, and O.S. Panasenko, Fiz. Metal. Metalloved., 38, no. 2, 438, (1974)

14 . K. Masui,S. Maruno, S. Sakakibara, T. Kawaguchi, J. Non-Cryst. solids, 74, 271, (1985)

15 . H. Masumoto, T. Kobayashi, and K. Watanabe, Trans. Japan Inst. Metals, 6, 187, (1965)

16 . J.E. Snyder, K.R. Mountfield, and M. H. Kryder, J. Appl. Phys. , 61(8), 3146, (1987)

17 . D.P. Ravipati, W.G. Haines, J.M. Sivertsen,J.H. Judy, J. Appl. Phys., 61, 3149, (1987)

18 . Y.Niimura, S. Nakagawa, Y. Kitamoto, and M. Nade, J. Appl. Phys., 61, 3152, (1987)

19 . J.A.Thompson, D.A. Stevensen, J.Appl.Phys., 61, 3155, (1987)

20 . S.Honda, N. Yamashita, M. Ohkoshi, and T. Kusuda, IEEE Trans. Magn., MAG-20 (5), 791, (1984)

21 . P.J. Grundy, M.Ali, J. Magn. and Magn. Mat., 40, 154, (1983)

22 . G. Hass and R.E. Thun, Physics of thin films, vo.3, Academic press, pp.34-, (1966)

23 . Practical electron microscopy in material science, vo.2, MacMillan, Philips tech. library, (1975)

24 . M.H. Loretto, Electron beam analysis of materials, Chapman and Hall, (1984)

25 . G. Thomas and M.J. Goringe, Transmission electron microscopy of materials, J. Wiley and sons, (1979)

26 . K. Ozawa, T. Yanada, H. Masuya, M. Sato, S. Ishio, M. Takahasi, J. magn. and magn. mat., 35, 289, (1983)

27 . J.S. Gau and W.E. Yetter, J. Appl. phys., 61, 3807, (1987)

28 . F.J. Cadieu, M.A. Russak, A.G. Pirich, J. magn. and magn. mat., 54, 1598, (1986)

29 . S.L. Zeder, J.F. Silvain, M.E. Re, M.H. Krudei, C.L. Bauer, J. Appl. phys., 61, 3804, (1987)

30 . T.R.Mcguire, J.A. Aboal, E. Klokholm, J.Appl. phys., 52(3), 2205, (1981)

31 . A.Tsoukatos, B.Dale, J.Strzeszewski, G.C.Hadjipanayis, to be published in Proc. of the 32nd annual MMM conf., (1987)

32 . A.Ovadia, I.B.Puchalska, J.P.Jakubovits, to be published in J. de Physique (1987)

MAGNETIC AND STRUCTURAL STUDIES OF Co-Al THIN FILMS AND BULK ALLOYS

by

A. G. TSOUKATOS

B.S., Concordia University, 1984
M.S., University of Manitoba,1986

AN ABSTRACT OF A THESIS

submitted in fulfillment of the

requirements for the degree

MASTER OF SCIENCE

PHYSICS

KANSAS STATE UNIVERSITY
Manhattan , Kansas

1988

ABSTRACT

Thin films of $Co_{100-x}Al_x$ were prepared by co-evaporation. The as-deposited films had the hexagonal Co structure for $x \leq 25$, a disordered bcc-CoAl structure for x=30, and a partially ordered bcc-CoAl structure for $x \geq 30$. After heat treatment at 650^0C the films with $x \leq 25$ changed microstructure to fine mixture of hcp-Co and an ordered fcc structure which may be interpreted as Co_3Al. Films with $25 \leq x \leq 50$ were transformed to ordered fcc- Co_3Al and bcc-CoAl structures after the heat treatment. The magnetization of the films was greater than that for bulk alloys with the same composition and it decreased when the films were annealed at 650^0C. The finely distributed two phase microstructure is probably responsible for the observed coercivity (50-150 Oe).

Ribbons of Co-Al were prepared by melt-spinning. The as melt-spun ribbons had a mixture of phases with a strong hcp-Co structure for $x \leq 25$, and strong hcp-Co and fcc-Co for $x \geq 25$. Co-rich phases continue to exist along with the Co_3Al phase in all of the compositions studied. The magnetization and coercivity values were comparable to those of bulk Co-Al of similar composition . The relatively high coercivities observed are attributed to the complex crystal structure found in all of the Co-Al ribbons.